Available online at www.sciencedirect.com
SCIENCE DIRECT
Polymer 46 (2005) 5308–5316
polymer
www.elsevier.com/locate/polymer

Melting behaviors and isothermal crystallization kinetics of poly(ethylene terephthalate)/mesoporous molecular sieve composite

Mingtao Run[a,b], Sizhu Wu[b], Dayu Zhang[b], Gang Wu[b,*]

[a]*Key Laboratory of Beijing City on 'Preparation and Processing of Novel Polymer Materials', Collage of Materials Science and Engineering, Beijing University of Chemical Technology, P.O. Box 90, Beijing 100029, People's Republic of China*
[b]*College of Chemistry & Environmental Science, Hebei University, Baoding 071002, HeBei Province, People's Republic of China*

Received 4 December 2004; received in revised form 12 April 2005; accepted 14 April 2005
Available online 28 April 2005

Abstract

Isothermal crystallization and subsequent melting behavior of mesoporous molecular sieve (MMS) filled poly(ethylene terephthalate) (PET) composites have been investigated at the designated temperature by using differential scanning calorimeter (DSC). The commonly used Avrami equation was used to fit the primary stage of the isothermal crystallization. The Avrami exponents n were evaluated to be $2 < n < 3$ for the neat PET and composites. MMS particles acting as nucleating agent in composite accelerated the crystallization rate with decreasing the half-time of crystallization. The crystallization activation energy calculated from the Arrhenius' formula was reduced as MMS content increased. It is shown that the MMS particles made the molecular chains of PET easier to crystallize during the isothermal crystallization process. Subsequent differential scanning calorimeter scans of the isothermally crystallized samples exhibited different melting endotherms. It is found that much smaller or less perfect crystals formed in composites due to the interaction between molecular chains and the MMS particles. The crystallinity of composites was enhanced by increasing MMS content.

Keywords: Mesoporous molecular sieve; Poly(ethylene terephthalate); Composite

1. Introduction

Poly(ethylene terephthalate) (PET) is a well established engineering plastic used in the manufacture of fiber, film and beverage containers, which derives from its good balance of thermal and mechanical properties. However, PET exhibits a relatively slow crystallization rate, which makes its application is limited in the field of injection molding. In order to control the crystallization rate and the crystallinity, and then achieve the desired morphology and properties, a great deal of efforts has been made on studying the crystallization kinetics corresponding to the change of the performed properties [1–8].

Recently, there has been much research on creating organic/inorganic composites by adding inorganic particles to the polymer matrix. The inorganic particles have contributed to greatly improving the crystallization, mechanical or rheological properties [9–14]. Various inorganic particles, such as montmorillonite, $CaCO_3$, SiO_2, TiO_2, etc. are usually used as filler in the polymer matrix to form the inorganic/organic composites. The benefit of the filling inorganic particles is to provide high rigidity with improving the yield strength or modulus, which mainly induce by the change of the crystallization of the polymer. Adequate amounts of inorganic usually promote the nucleation with increasing the crystallization rate of PET. At the same time it reduces the specific free energy of the nucleus formation during crystallization.

Mesoporous zeolite has been receiving much attention since the 1990s [15,16]. Mesoporous materials can be used as adsorbents [17], supports [18] and catalysts [19], etc. The mesoporous molecular sieve (MMS) is a main species that has been investigated by many researchers due to its particular characteristics, such as large internal surface area, uniform framework and easily controlled pore diameter from 2 to 10 nm [15,16]. With the different synthesizing and/or post-treat methods, the MMS particles can be

* Corresponding author. Tel.: +86 10 64444923; fax: +86 10 64437587.
E-mail addresses: gangwubuct@ sina.com (G. Wu), rmthyp@hotmail.com (M. Run).

0032-3861/$ - see front matter © 2005 Elsevier Ltd. All rights reserved.
doi:10.1016/j.polymer.2005.04.031

tailored with a size of nanometer order to a few submicron meters in the external diameter [20]. Several researches have been investigated the mesoporous materials as nanoreactor for organic monomers to polymerize into polymers [21–24]. Kageyama [24] prepared polyethylene (PE) within MCM-41 channel in a linear form, which has high molecular weight with few branch chains and show particular crystallization properties. Kojima [25] prepared nylon 66/mesoporous molecular sieve composite by annealing the mixtures of nylon 66 and mesoporous molecular sieve particles under high pressure and high temperature. However, since the polymerization reactions have happened within the mesopore channel, there have been few researches related to the composite of PET/MMS or its isothermal crystallization behaviors.

Some polymer/MMS composites have been prepared by the in situ polymerization with different MMS contents in our previous study, and their mechanical properties has been found to be improved with increasing MMS content. Moreover, some polymers have been formed within the mesoporous channels proved by experiments [26]. As a further study, the melting behavior, isothermal crystallization kinetics and spherulite morphology of the PET/MMS composite are investigated in this article. The isothermal crystallization process is adopted to investigate the effect of submicron-particles in PET matrix. From DSC measurements, the study on the isothermal crystallization kinetics is performed through the Avrami equation [27]. The crystallization activation energy is also investigated by Arrhenius method.

2. Experimental

2.1. Materials

The details of MMS particles prepared by the ultrasonic synthesis had been described previously [28] and its characteristics were listed in Table 1. MMS particles were outgassed at 120 °C under vacuum for more than 2 h. Ethylene glycol (EG,99%), terephthalic acid (TPA,99%) and bishydroxyethyl terephthalate (BHET) were obtained from Yanshan Sinopec Co. Phenol and tetrachloroethane (TCE,97%) were produced by Beijing Chemical Co.

The PET/MMS composites were prepared by in situ esterification and a following polycondensation in the molten state with BHET, EG and dried MMS as the reaction materials. Sb_2O_3 (0.03 wt%) and phosphorus were added into the system as the catalyst and stabilizer, respectively. The preparation of neat PET was similar to that of PET/MMS composites but without the MMS additive. All the molten products was quenched by cold water and then cut into pellet. The products were dried in a vacuum oven at 140 °C for 12 h before determining the viscosity and being used in DSC measurements. Corresponding to the weight percentage of MMS, the products were named as neat PET (MMS 0%), PET1 (MMS 1 wt%), PET2 (MMS 2 wt%) and PET4(MMS 4 wt%) as shown in Table 2.

The intrinsic viscosity [η_{rel}], was measured in a solution of phenol/tetrachloroethane (50/50 w/w) at 25 °C by using Ubbelohde viscometer. The [η_{rel}] of PET, PET1, PET2 and PET4 was found to be 0.60, 0.57, 0.56 and 0.59 dl/g, respectively.

2.2. Analysis

The melting and crystallization behavior of four samples were investigated by the following program: the dried samples were first heated at a heating rate of 80 °C/min from room temperature to 290 °C, held there for 5 min and then cooled to 50 °C at a rate of 160 °C/min to obtain amorphous state samples; then heated again at a rate of 10 °C/min to 290 °C, held there for 5 min and cooled to 50 °C at a rate of 10 °C/min. The second heating and cooling process were recorded by the Perkin–Elmer DSC-7 instrument.

The isothermal crystallization and melting process were performed as following: the samples were heated at a rate of 80 °C/min to 290 °C, held for 5 min and then cooled to the designated crystallization temperatures (T_c) rapidly (160 °C/min). After the isothermal crystallization finished, the samples were heated to 280 °C at a rate of 10 °C/min.

Samples for polarized optical microscopy (POM) measurement were prepared by sandwiching a tiny pellet of PET/MMS composite between two glass plates, compressing at 270 °C for 5 min and then annealing in an oven at 210 °C for 3 h. POM observation was performed by Leitz SM-LUX-POL.

3. Results and discussion

3.1. Melting and crystallization behavior

Fig. 1 gives DSC curves of the four samples. The kinetic parameters of the melting process are summarized in Table 2. It is shown that the neat PET exhibits an apparent glass

Table 1
Characteristics of the MMS sample

Sample	Unit-cell parameter (nm)		BET surface area ($m^2\ g^{-1}$)	Pore size (nm)	Pore volume ($cm^3\ g^{-1}$)	Wall thickness (nm)	Average particle size (μm)
	d_{100}	α_0					
MMS	3.93	4.54	1119	2.93	1.123	1.61	0.35

Table 2
Kinetic parameters of melting and crystallization for various samples

Sample	Heating scan					Cooling scan	
	T_g (°C)	$T_{c,c}$[a] (°C)	ΔH_c[b] (J/g)	T_m (°C)	ΔH_m (J/g)	$T_{c,h}$[c] (°C)	ΔH (J/g)
PET	79.5	151.2	−37.4	252.3	45.9	190.0	−41.8
PET1	85.2	–	–	253.7	44.4	207.7	−48.9
PET2	87.6	–	–	255.0	43.1	209.3	−45.9
PET4	89.5	–	–	256.8	39.7	211.4	−44.9

[a] The temperature of cold crystallization peak in the heating scan.
[b] The cold crystallization enthalpy in the heating scan.
[c] The temperature of melt-crystallization peak in the cooling scan.

transition at about 79 °C, a cold crystallization peak at about 151 °C, and a melting peak at about 252 °C.

In the cases of samples PET1, PET2 and PET4 including an increased MMS, however, neither obvious glass transition nor the cold crystallization is observed in their DSC diagrams. By careful observation, it is recognized that the melting peak shifts to a higher temperature gradually with the increased content of MMS. The cold crystallization peak area is smaller than the melting peak area of neat PET, which indicates that at the cooling rate of 160 °C/min, the molten PET molecules are frozen at the amorphous state directly. While molten PET1 and PET2 are essentially turned into a semicrystalline one at the same cooling rate.

The crystallization behavior of four composite samples at the cooling rate of 10 °C/min from melting state is shown in Fig. 2, and the kinetic parameters of the cooling process are summarized in Table 2. It can be seen that at this cooling rate, the crystallization exothermal peak is gradually shifted to high temperature with increased content of MMS. The half-peak width is narrowed as the MMS content is increased. Compared the $T_{c,h}$ of PET and PET1, the crystallization temperature is raised 17.7 °C (Table 2) by only adding 1 wt% MMS in composite. These results indicate that the MMS particles can increase the melt-crystallization temperature and the crystallization rate dramatically, and show that this agent may be an ideal nucleating agent for PET processing.

3.2. Isothermal crystallization kinetic analysis

3.2.1. Isothermal crystallization behaviors

The exothermal diagrams of isothermal crystallization analysis for PET and PET/MMS composites are shown in Fig. 3(a)–(c). As the crystallization temperature (T_c) increases, the exothermal peaks of each curve are shifted to longer time, indicating that the T_c is an important influencing factor determining the crystallization time. From the data listed in Table 3, the crystallization enthalpy (ΔH) of neat PET increases greatly, implying that the total crystallization increases with increasing T_c. While for PET1 and PET2, the peaks location and enthalpy change slightly with increasing T_c, indicating a minor dependence on T_c. These results suggest that the MMS content has been a predominant influencing factor determining the crystallization time, and the crystallization rate of the composites is raised by MMS particles, while the T_c only have a secondary impact on the crystallization time.

Fig. 4(a)–(c) shows the relative crystallinity (X_t) integrated from Fig. 3 as a function of the crystallization time (t) for samples PET, PET1 and PET2 at various isothermal crystallization temperatures (T_c). In Fig. 4(a)–(c), the characteristic sigmoidal isotherms are shifted to right along the time axis with increasing T_c. This result indicates a progressively slower crystallization rate as T_c increases.

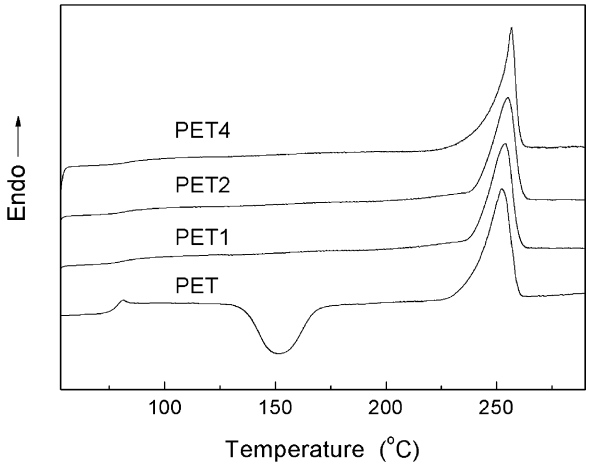

Fig. 1. Melting DSC curves of four composites.

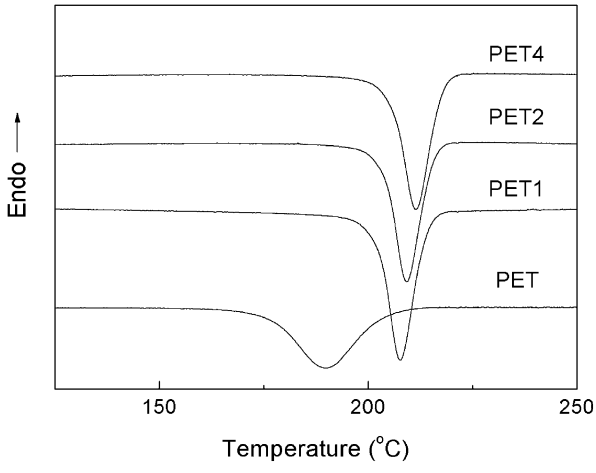

Fig. 2. Melt-crystallization DSC curves of four composites.

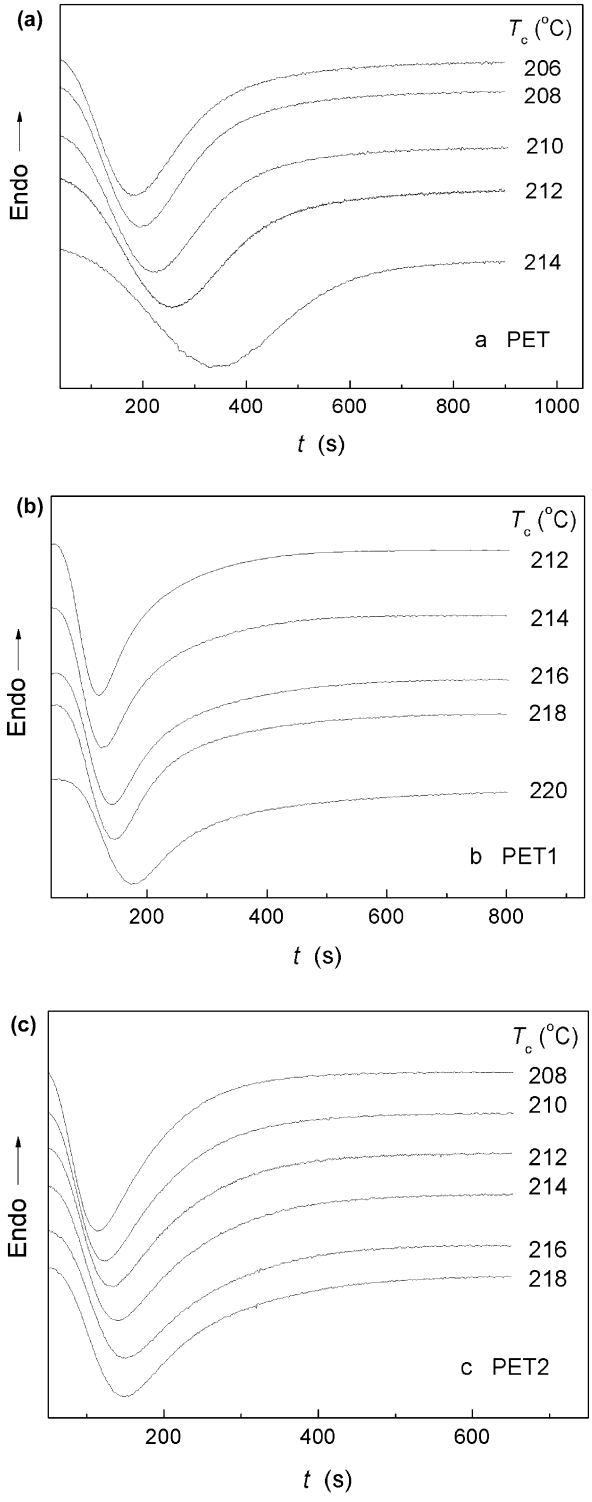

Fig. 3. Heat flow versus time during isothermal crystallization of (a) PET, (b)PET1 and (c)PET2 composites at different crystallization temperatures by DSC.

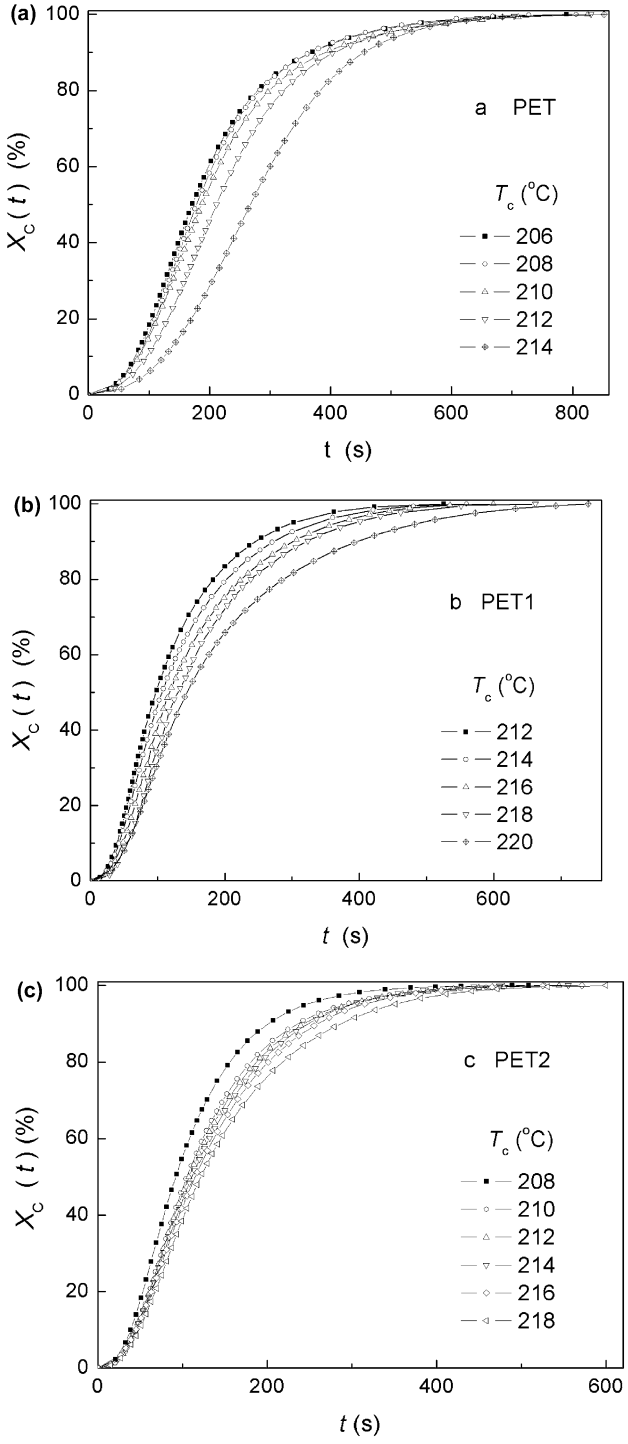

Fig. 4. Development of relative degree of crystallization X_c with time t for isothermal crystallization of (a) PET, (b) PET1 and (c) PET2 composites at different crystallization temperatures.

Another important parameter is the half-time of crystallization ($t_{1/2}$), which is defined as the time taken from the onset of the relative crystallization until 50% completion. The dependence of $t_{1/2}$ upon T_c for various samples is shown in Fig. 5 and also listed in Table 3. It is observed that $t_{1/2}$ of the neat PET increases sharply as T_c increased from 206 to 214 °C, indicating that the neat PET is the thermal-activated crystallization polymer. Whereas PET1, PET2 and PET4 show slowly changes of $t_{1/2}$ with increasing T_c and the lower dependency characteristic on T_c than the neat polymer. As

Table 3
Kinetic parameters of isothermal crystallization for various samples

Sample	T_c (°C)	n	$Z_t \times 10^6 (s^{-n})$	$t_{1/2}$ (s)	ΔH (J/g)
PET	206	2.5	2.21	172	−18.3
	208	2.5	1.69	180	−21.2
	210	2.5	1.79	188	−28.9
	212	2.4	1.67	211	−30.6
	214	2.4	1.23	269	−31.2
PET1	212	2.4	14.1	98	−32.6
	214	2.4	14.3	107	−32.9
	216	2.4	13.8	119	−33.6
	218	2.3	13.3	131	−33.0
	220	2.2	12.7	150	−31.8
PET2	208	2.4	16.0	93	−33.2
	210	2.4	12.1	105	−34.9
	212	2.4	13.2	108	−33.1
	214	2.3	15.8	111	−32.8
	216	2.2	21.6	116	−31.0
	218	2.3	14.0	123	−34.3

$T_c = 212$ or 214 °C (Table 3), $t_{1/2}$ of the neat PET is evidently longer compared to that of PET1 and PET2. From the above results, a clearly increase of crystallization rate has been occurred as MMS content increases in PET matrix.

3.2.2. Analysis based on the Avrami equation

Assuming that the relative crystallinity (X_t) increases with the crystallization time (t), the Avrami equation can be used to analyze the isothermal crystallization process of the neat PET and PET/MMS composites as follows [27,29]:

$$1 - X_c(t) = \exp(-Z_t t^n) \quad (1)$$

$$\log[-\ln(1 - X_c(t))] = n \log t + \log Z_t \quad (2)$$

where $X_c(t)$ is the relative degree of crystallinity at time t; the exponent n is a mechanism constant with a value depending on the type of nucleation and the growth dimension, and the parameter Z_t is a growth rate constant involving both nucleation and the growth rate parameters.

The plots of $\log[-\ln(1-X_c(t))]$ versus $\log t$ according to Eq. (2) are shown in Fig. 6(a)–(c). The crystallization process is usually treated as two stages: the primary crystallization stage and the secondary crystallization stage. In Fig. 6, one can see that each curve is composed of two linear sections. This fact indicates that the existence of the secondary crystallization of the neat PET and PET/MMS composites. It is generally believed that the secondary crystallization was caused by the spherulite impingement in the later stage of crystallization process [29–32]. By comparing three curves measured at the same temperature, e.g. $T_c = 212$ °C as seen in Fig. 6(a)–(c), the occurring time of secondary crystallization of PET1 and PET2 are $t = 80$ s ($\log t = 1.90$) and $t = 76$ s ($\log t = 1.88$), respectively. These are much shorter than the neat PET ($t = 200$ s, $\log t = 2.3$). This fact indicates that without the intervention of MMS, the nucleus in the neat PET grow slowly into spherulites before they impinge against each other. MMS cause primary crystallization completed earlier because much small crystals or microcrystallites form rapidly and then impinge against each other.

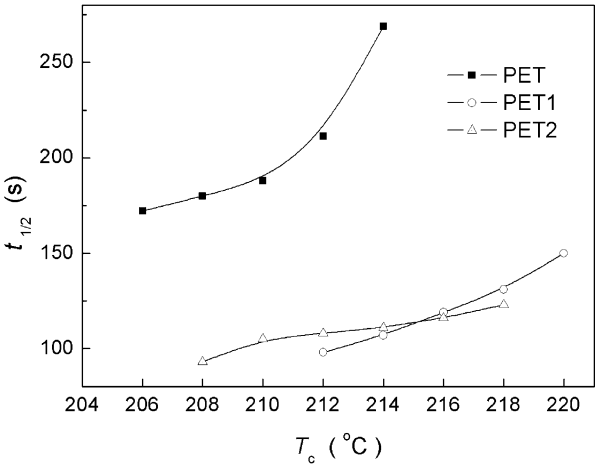

Fig. 5. The $t_{1/2}$ versus T_c of isothermal crystallization for various PET/MMS composites.

The Avrami exponent n and the rate constant Z_t can readily be extracted from the Avrami plots in Fig. 6. The values of n and Z_t of various samples are listed in Table 3. In this work, the values of n are between 2 and 3 for the neat PET, PET1 and PET2, which are about 2.5 ± 0.1, 2.3 ± 0.1 and 2.3 ± 0.1, respectively. It may be an average value of various nucleation types and the growth dimensions occurred simultaneous in a crystallization process. As $T_c = 214$ °C (Table 3), the n values slightly decrease with increasing MMS content at primary crystallization stage. For neat PET without any heterogeneous nucleus, its nucleation type should predominantly be homogenous nucleating and its growth dimensions should predominantly be a two-dimensional growth. For PET1 and PET2 with heterogeneous nucleus MMS, its nucleation type should mostly be heterogeneous nucleating and its growth dimension should mostly be two-dimensional space extension.

The crystallization rate parameters (Z_t) of the neat PET,

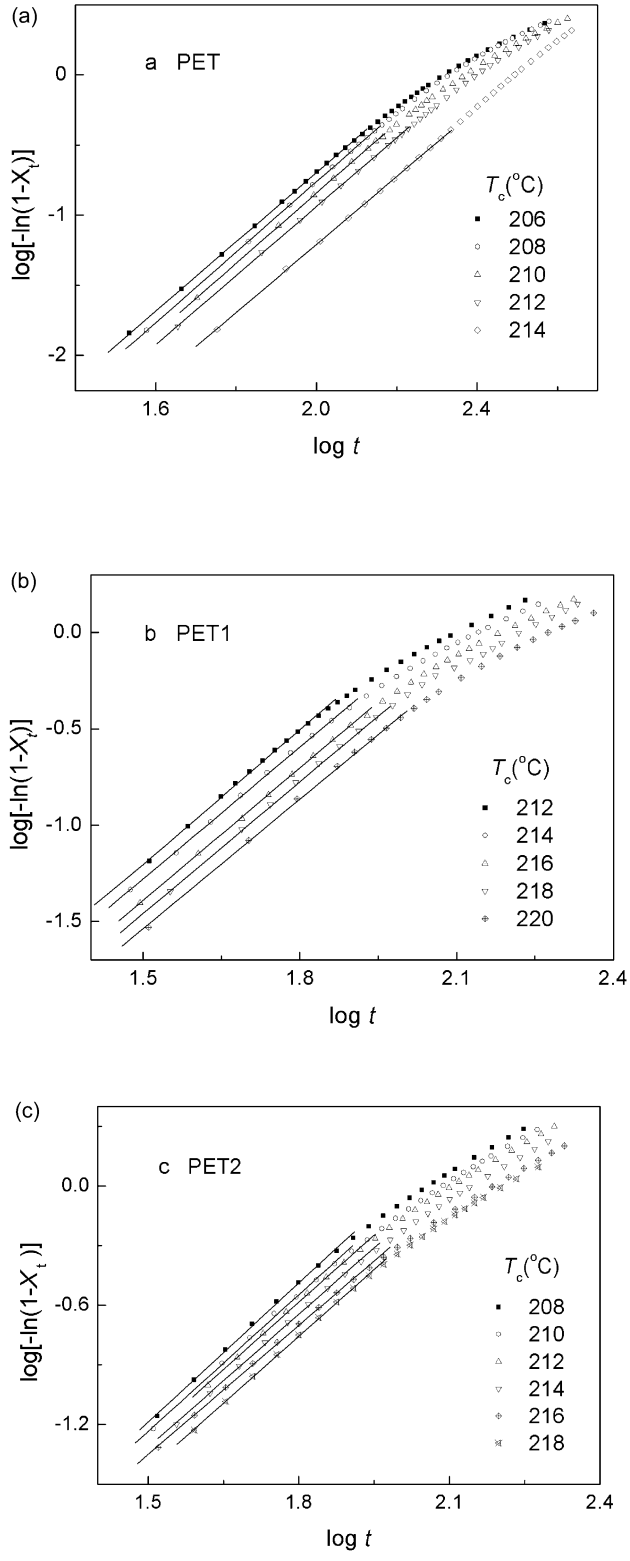

Fig. 6. Plots of $\log[-\ln(1-X_c(t))]$ versus $\log t$ for (a) PET, (b) PET1 and (c) PET2 composites of isothermal crystallization at indicated temperatures.

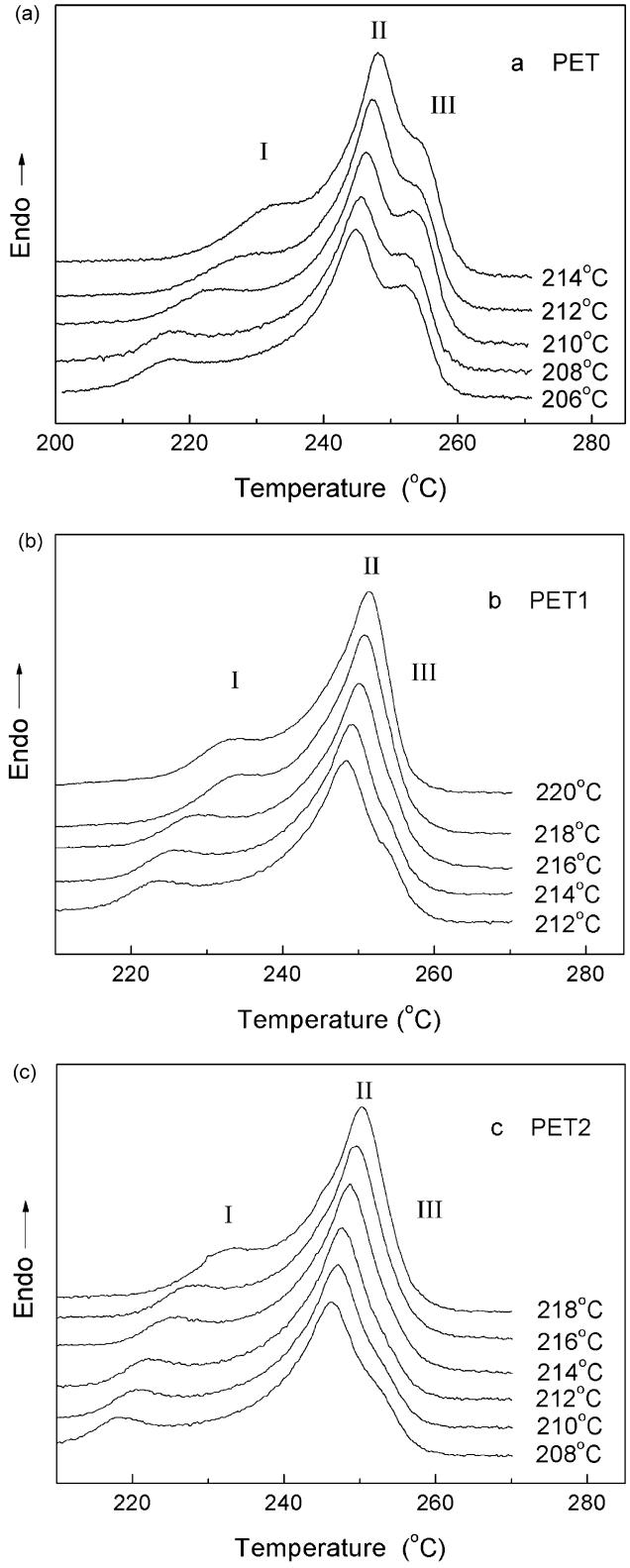

Fig. 7. Melting endotherms of (a) PET, (b) PET1 and (c) PET2 composites recorded at a heating rate of 10 °C/min, after isothermal crystallization at the specified temperature.

PET1 and PET2 at $T_c = 214$ °C are also listed in Table 3 and compared each other. Z_t of PET1 increase about ten times to the one of the neat PET, and Z_t of PET2 is further higher than that of PET1. These facts indicate that the more MMS nucleating agents in composites, the faster crystallization rate.

3.2.3. Melting behavior of the samples annealed at different temperatures

Fig. 7(a)–(c) present a series of DSC heating thermograms of the neat PET and PET/MMS composites that are annealed at different T_c. The melting parameters are summarized in Table 4. From both Fig. 7(a) and Table 4, it is apparent that the neat PET endotherms exhibit three melting peaks. These peaks are shifted to higher temperature as T_c increases. Peak I is shifted more sharply to high temperature than other two peaks. Apparently, peak II and peak III are tended to combine together with increasing T_c from 206 to 214 °C. According to similar explanations of multiple endotherms of PET [33–36], these peaks mainly refer to the melting of the crystals with different crystal perfection. The cause of peak I is assumed to be microcrystallite formation in the boundary layer between the larger crystallites. Peak II corresponds to the primary crystal with perfect form; while peak III is attributed to the melting of the furthest perfect crystals. As T_c increases, the melting endotherms are shifted to higher temperature, indicating that more perfect crystals have formed at higher T_c. As seen in Fig. 7(a) where the area of peak II is larger than either of peak I or III, indicating that the major crystallization of the polymer is predominantly composed of the primary crystals.

As seen in Fig. 7(b) and (c), all the melting endotherms of PET1 and PET2 only exhibit two primary melting peaks. By comparing the melting endotherms of the neat PET with that of PET1 and PET2 at the same temperature, e.g. $T_c =$ 212 °C, peak III of the neat PET is observed obviously a shoulder shape; while the peak III of PET1 is very small although it is still observed in its endothermal trace. The peak III of PET2, however, is difficult to observe in its endothermal trace. These results indicate that the number of furthest perfect crystals decreases with increasing MMS content. Furthermore, as $T_c = 212$ °C (Table 4), the temperature of peak I is varied with various MMS content, and their values are 228.2 °C (PET), 224.0 °C (PET1) and 222.1 °C (PET2), respectively. Therefore, it might be concluded that the MMS particles can improve the formation of the microcrystallite with poor morphology. This fact is confirmed with the result in Fig. 6, which the impingement of the poor microcrystallites caused the secondary crystallization stage occurred earlier. According to the values of X_c in Table 4, the crystallinity is also enhanced with increasing MMS content in PET at the same T_c.

After annealing at 210 °C for 3 h, the crystals morphology of PET and PET1 are observed by polarizing microscope and two microphotographs are shown in Fig. 8. For neat PET, spherulites are fairly big and perfectly grown with the maltese cross clearly observed. PET1 composite has uniform microcrystallites without big or perfectly maltese cross. The primary spherulites of PET are about 10–15 times larger than those of PET1 composite. This result may indicate that MMS particles in PET1 composite have been served as seeds for spherulites growth, and the crystals may grow on the surface of the MMS particles. As the spherulites grow, they may be confined by each other and the MMS particles as well, so they are fine and uniform, but not as big as in neat PET.

3.2.4. Crystallization activation energy

The crystallization process of the neat PET and PET/MMS composites is assumed to be thermally activated.

Table 4
Melting endotherms parameters of various samples

Sample	T_c (°C)	T_m (°C)			ΔH_f (J/g)	X_c[a] (%)
		I	II	III		
PET	206	217.2	245.0	252.2	38.0	27.1
	208	218.2	245.7	252.2	38.4	27.4
	210	224.7	246.3	253.1	42.4	30.3
	212	228.2	247.2	253.5	41.4	29.6
	214	231.5	248.1	254.0	44.0	31.4
PET1	212	224.0	248.4	253.2	45.2	32.3
	214	225.6	249.2	253.4	44.9	32.1
	216	228.0	249.9	–	48.7	34.8
	218	233.0	250.8	–	48.7	34.8
	220	233.2	251.2	–	48.7	34.8
PET2	208	217.7	246.4	251.6	45.3	32.4
	210	220.6	247.1	–	45.7	32.7
	212	222.1	248.5	–	46.3	33.1
	214	225.3	248.7	–	48.5	34.6
	216	227.5	249.5	–	51.1	36.5
	218	233.4	250.2	–	54.0	38.6

[a] X_c is calculated from formula: $X_c = (\Delta H_f/\Delta H_f^0) \times 100$, $\Delta H_f^0 = 140$ J/g.

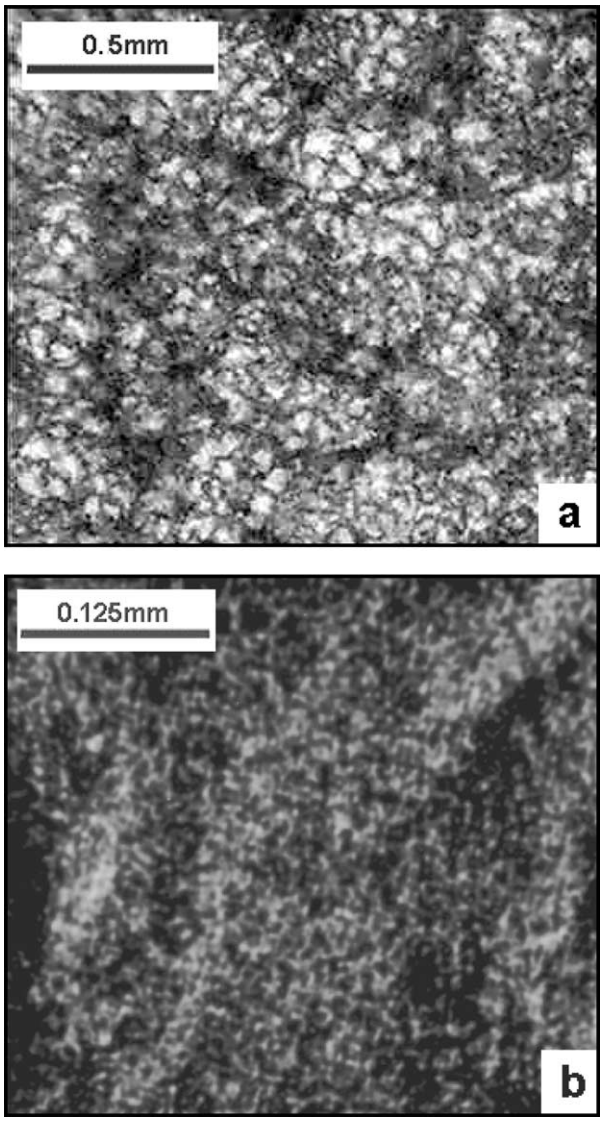

Fig. 8. Polarizing microscope of crystallization (a) PET and (b) PET1 composites.

The crystallization rate parameters Z_t can be approximately described by the following Arrhenius equation [37]:

$$Z_t^{1/n} = Z_0 \exp\left(\frac{-\Delta E}{RT_c}\right) \tag{3}$$

$$\left(\frac{1}{n}\right)\ln Z_t = \ln Z_0 - \frac{\Delta E}{RT_c} \tag{4}$$

where Z_0 is the temperature independent pre-exponential factor, R is the gas constant, and ΔE is the crystallization activation energy. ΔE can be determined by the slop coefficient of plots with $(1/n)\ln Z_t$ versus $1/T_c$ in Eq. (4) which shown in Fig. 9. Because it has to release energy when the molten fluid transformed into the crystalline state, the value of ΔE is negative on the basis of the concept of the heat quantity in physical chemistry. In this study, the ΔE value for various samples in primary crystallization stage is

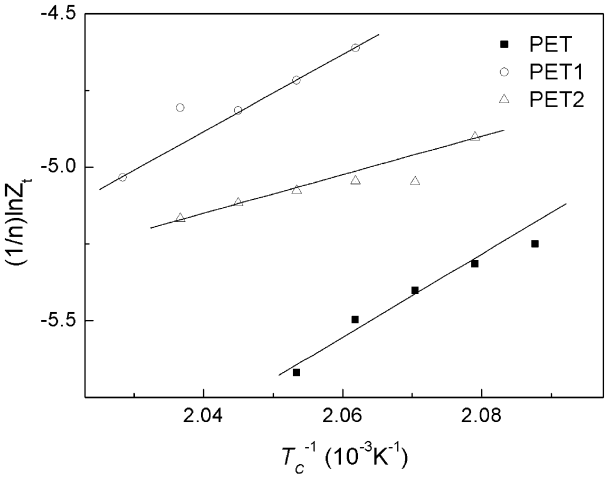

Fig. 9. Plot of $(1/n)\ln Z_t$ versus $1/T_c$ for Avrami parameter Z_t deduced from isothermal crystallization.

found to be −112.9 (PET), −104.8 (PET1), and −52.3 (PET2) kJ/mol, respectively. This result suggests that the crystallization activation energy of the composites decreases as MMS content increases. From the above results, the MMS particles make the molecular chains of PET easier to crystallize, and accelerate the crystallization rates during isothermal crystallization process.

Although increase of crystallization rate and reduction of crystallization activation energy are common characteristics for polymer/nano-particles composites, the MMS particles have different influence on crystallization process of PET/MMS composites compared to the organic modified layered silicates or other inorganic particles with only the external surface. The organic modified layered silicates, e.g. organoclay, are exfoliated and dispersed homogeneously in the polymer matrix to form exfoliated nanocomposites. The sheet nanolayers can easily absorb the polymer segments on its external surface, and this strong interaction between polymer chains and the layer leading to a nucleation effect in the crystallization process. While, the spherical MMS particles have large internal surface, pore volume and pore size, therefore, not only the external surface but also the internal surface of the MMS particles are covered with the polymers after the in situ polymerization. The polymers in the nano-channel are adsorbed by the internal surface and confined by the pore wall. Furthermore, some polymer chains will extend out from the nano-channel to the matrix, entangling with the polymer chains of the matrix. These structure characteristics may improve the interaction between the MMS particles and the polymer. As a result, the nucleation effect may occur greatly.

4. Conclusion

PET/MMS composites are prepared by the in situ polymerization to raise the crystallization rate, the degree

of crystallinity and the glass transition temperature of PET. The Avrami analysis indicates that the crystallization process is composed of the primary stage and the secondary stage. At the primary stage, the Avrami exponent n decreases slightly as the MMS content increases. The crystallization rate increases much with increasing MMS content. The secondary crystallization stage occurs earlier with increasing MMS content. The crystallization activation energy is reduced as the MMS content increases, and MMS particles make PET easier to crystallize during isothermal crystallization process.

Observation of subsequent melting endotherms of the composites after isothermal crystallization at the specified crystallization temperatures shows multi-melting peaks. MMS particles cause a decreasing of the furthest perfect crystals at high temperature and an increasing of micro-crystallites at lower temperature in composite. This result is also confirmed by the POM results with many smaller uniform spherulites. The degree of crystallinity is enhanced gradually by MMS content. Therefore, MMS particles have been successfully acted as nucleation agents in the PET matrix, and the crystallization properties is improved greatly.

Acknowledgements

This study was supported by China SINOPEC Corp. under project X503013.

References

[1] Ozawa T. Polymer 1971;12:150.
[2] Van Antwerpen F, Van Krevelen DW. J Polym Sci, Polym Phys 1972; 10:2423.
[3] Gunther B, Zachmann HG. Polymer 1983;24:1008.
[4] Zhou CX, Clough SB. Polym Eng Sci 1988;28:65.
[5] Balta-Calleja FJ, Santa Cruz C, Asano T. J Polym Sci, Polym Phys 1993;31:557.
[6] Lu X, Hay JN. Polymer 2001;42:9423.
[7] Avila-Orta CA, Medellín-Rodríguez FJ, Wang ZG, Navarro-Rodríguez D, Hsiao BS, Yeh F. Polymer 2003;44:1527.
[8] Lee B, Shin TJ, Lee SW, Yoon J, Kim J, Youn HS, Ree M. Polymer 2003;44:2509.
[9] Fann DM, Huang SK, Lee J. J Polym Eng Sci 1988;38:265.
[10] Evstatiev M, Fakirov S. Polymer 1992;33:877.
[11] Xu W, Ge M, He P. J Appl Polym Sci 2001;82:2281.
[12] Yang H, Cao J, Ao W, Qiu G. Polym Mater Sci Eng 2003;19(3):68.
[13] Arkhireeva A, Hay JN. Polym Polym Compos 2004;12:101.
[14] Chang J, Kim SJ, Joo YL, Im S. Polymer 2004;45(3):919.
[15] Kresge CT, Leonowicz ME, Roth WJ, Vartuli JC, Beck JS. Nature 1992;359:710.
[16] Beck JS, Vartuli JC, Roth WJ, Leonowicz ME, Kresge CT, Schmitt KD, et al. J Am Chem Soc 1992;114:10834.
[17] Branton PJ, Hall PG, Sing KSW. J Chem Soc, Chem Commun 1993;1275.
[18] Corma A, Martinez A, Soria VM, Monton JB. J Catal 1995;153:25.
[19] Mobil Oil Corp. Synthetic porous crystalline material and preparation. Useful as sorbent or catalyst component with hexagonal arrangement of uniformly-sized pores, WO Patent 1991;9,111,390A.
[20] Yao YF, Zhang MS, Yang YS. Acta Phys-Chim Sin 2001;17(12): 1117.
[21] Wu CG, Bein T. Science 1994;264:1757.
[22] Wu CG, Bein T. Science 1994;266:1013.
[23] Moller K, Bein T, Fischer RX. Chem Mater 1999;11:665.
[24] Kageyama K, Tamazawa J, Aida T. Science 1999;285:2113.
[25] Kojima Y, Matsuoka T, Takahashi H. J Appl Polym Sci 1999;74: 3254.
[26] Wu G, Run M., Zhang D. in preparation.
[27] Avrami M. J Chem Phys 1940;8:212.
[28] Run M, Wu S, Wu G. Microporous Mesoporous Mater 2004;74:37.
[29] Avrami M. J Chem Phys 1939;7:1103.
[30] Wunderlich B. Macromolecular physics. vol. 2. New York: Academic Press; 1977.
[31] Liu JP, Mo ZS. China Polym Bull 1991;4:199.
[32] Liu T, Mo Z, Wang S, Zhang H. Polym Eng Sci 1997;37(3):568.
[33] Roberts RC. J Polym Sci B 1970;8:381.
[34] Sweet GE, Bell JP. J Polym Sci A-2 1972;10:1273.
[35] Lu XF, Hay JN. Polymer 2001;42:9423.
[36] Kong Y, Hay JN. Polymer 2003;623.
[37] Cebe P, Hong SD. Polymer 1986;27:1183.